Dose Rate Evaluation for the ES-3100 Package with HEU Content Using MCNP, ADVANTG, Monaco, and MAVRIC

Pran K. Paul*

Consolidated Nuclear Security, LLC (CNS), Y-12 National Security Complex
P.O. Box 2009, Oak Ridge, Tennessee 37831-8163

* Email: pran.paul@cns.doe.gov

Number of pages: 32

Number of tables: 7

Number of figures: 18

DISCLAIMER

Abstract

This paper presents a comparative study of dose rate calculations for the ES-3100 package with highly enriched uranium (HEU) content for different source configurations using computer codes: (1) MCNP; (2) Automated Variance Reduction Generator (ADVANTG)/MCNP; (3) Monaco; and (4) Monaco with Automated Variance Reduction using Importance Calculations (MAVRIC). The Model ES-3100 package was developed at the Y-12 National Security Complex for domestic and international transportation of Type B fissile radioactive material. In this study, six different source configurations (i.e., solid cylinder, cylindrical hemi-shell, cylindrical shell, rectangular plate, cylindrical rod, or cylindrical segment form) having 36 kg of HEU metal inside the package containment vessel (based on configurations in the ES-3100/HEU safety analysis report for packaging) are evaluated. Dose rates at the package surfaces and 1 m from the package surfaces are calculated for these different source configurations. MCNP and Monaco cases are run without any biasing options to accelerate the convergence. Consistent Adjoint Driven Importance Sampling (CADIS) and Forward-Weighted CADIS (FW-CADIS) methods developed at the Oak Ridge National Laboratory are implemented in ADVANTG/MCNP and MAVRIC codes to accelerate the convergence. ADVANTG generates variance reduction parameters using Denovo code, and MCNP is used with the variance reduction parameters to accelerate the convergence. MAVRIC uses Denovo code to construct an importance map and a biased source distribution that are supplied to Monaco to accelerate the Monte Carlo simulation. The FW-CADIS option in ADVANTG and MAVRIC is used to accelerate the convergence in this study. The accelerated convergence cases (ADVANTG/MCNP and MAVRIC) are about 100 times faster with 100 times less particle simulation than those cases run without biasing options (analog MCNP and analog Monaco). The MCNP, ADVANTG/MCNP, Monaco, and MAVRIC calculated dose rates at the package surfaces and at 1 m from the package surfaces for the different source configurations are compared and are found to be in general agreement.

Keywords — Monte Carlo calculation, shielding evaluation, ES-3100 package

I. INTRODUCTION

This paper presents a comparative study of dose rate calculations at the package surfaces and 1 m from the package surfaces for the ES-3100 package with highly enriched uranium (HEU) content [1] for different source configurations using shielding evaluation computer codes: MCNP [2], Automated Variance Reduction Generator (ADVANTG)/MCNP [3], Monaco, and Monaco with Automated Variance Reduction using Importance Calculations (MAVRIC) [4]. MCNP is a general purpose Monte Carlo code developed at the Los Alamos National Laboratory (LANL) for shielding analysis. ADVANTG is an automated variance reduction parameter generator code developed at the Oak Ridge National Laboratory (ORNL) for MCNP applications. ADVANTG generates space- and energy-dependent mesh-based weight-window bounds and biased source distributions from three-dimensional (3-D) block-parallel discrete ordinate (S_N) calculations that are performed by Denovo [5] computer code developed at ORNL. Monaco and MAVRIC codes are part of the SCALE code system developed at ORNL for shielding analysis. Chapter 5 of the ES-3100/HEU safety analysis report for packaging (SARP) [1] documents the shielding evaluation for the contents in the package based on MCNP calculations without using any of the inherent variance reduction techniques. The dose rates are calculated on the package surfaces for normal conditions of transport (NCT) and at 1 m from the package surfaces for NCT and hypothetical accident conditions (HAC) as defined in Title 10 of the Code of Federal Regulations (CFR), Part 71 (10 CFR 71) [6], and 49 CFR [7]. The dose rates are compared with the regulatory limits to show that there is sufficient margin between the calculated dose rates and the regulatory limits. The MORSE code updated by ORNL and called Monaco is now part of the SCALE code system. The MAVRIC sequence is also available as part of the SCALE code system. MAVRIC uses Denovo code in SCALE to construct an importance map and a biased source distribution, which are supplied to Monaco to accelerate the convergence in dose rate calculations.

This paper presents a comparative study of dose rates for the NCT conditions for different source configurations used in the ES-3100/HEU SARP. The source configurations analyzed are: solid cylinder at the top and bottom of the containment vessel (CV), cylindrical hemi-shell, cylindrical shell, rectangular

plate, cylindrical rod, and cylindrical segment. The HAC dose rates are historically much lower than the regulatory limits for packages. As a result, the HAC dose rates are not included in this study.

Several Type B fissile-material packages have been developed at the Y-12 National Security Complex (Y-12) for transportation of radioactive materials, and Y-12 personnel have been involved in the design, testing, and certification of fissile-material packages for more than 30 years. Packages are being developed to replace older packages that do not conform to the current requirements specified in 10 CFR 71 [6]. Safety basis documentation termed a SARP is prepared to certify a particular packaging with specified contents. The contents are typically unirradiated or slightly irradiated uranium or plutonium metals and oxides. The purpose of the SARP is to demonstrate compliance with U.S. Nuclear Regulatory Commission regulatory requirements specified in the 10 CFR 71 and U.S. Department of Transportation requirements specified in 49 CFR for safe transportation of radioactive materials. Once a SARP is approved, a certificate is issued from the regulatory agency for the package. The ES-3100 package is an example of a Type B fissile material package developed at Y-12 to transport HEU metal and oxide contents.

II. DESCRIPTION OF THE ES-3100 TRANSPORTATION PACKAGE

The Model ES-3100 packaging, which is shown as a sectional view in Fig. 1 (a), has two major systems, a drum assembly and a CV. The drum assembly consists of an outer drum, impact-absorbing and thermal-insulating material, an inner liner, and a top plug. The CV consists of a pressure vessel with associated lid and O-ring seals. Figure 1 (b) shows the schematic of the ES-3100 packaging with the dimensions of various components. The ES-3100 package for NCT consists of stainless-steel convenience cans loaded with HEU material, can spacer assemblies to support and position the convenience cans, the CV, and an insulation-filled drum. The impact-absorbing and thermal-insulating material is Kaolite 1600, which is a mixture of Portland cement and expanded vermiculite. Another significant feature of the drum assembly is the neutron-absorbing material 277-4 (or Cat 277-4 as it is sometimes referred) that is cast into the innermost liner of the packaging adjacent to the CV as shown in Fig. 1. For NCT and HAC shielding calculations, the packing materials inside the CV are conservatively not modeled. During HAC, it is

assumed that the CV remains intact, but packaging materials external to the CV are removed. The geometry of the shielding analysis model is a conservative, cylindrical representation of the package. In this study, only the NCT dose rates calculated by analog MCNP, ADVANTG/MCNP, analog Monaco, and MAVRIC are analyzed.

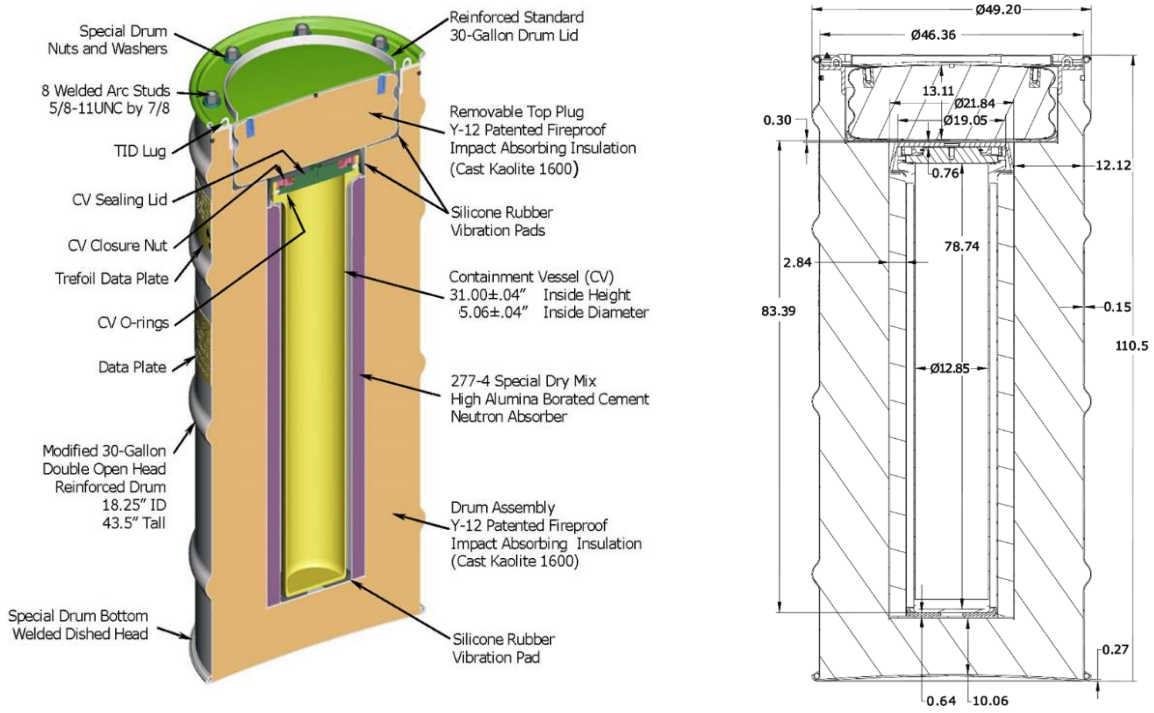

(a) (b)

Fig. 1. ES-3100 packaging (a) section view of the packaging components and (b) schematic (dimensions in cm).

III. OVERVIEW OF THE COMPUTER CODES USED

MCNP [2] is a general purpose Monte Carlo code developed at the LANL that can be used for multidimensional neutron, photon, or coupled neutron/photon transport calculations, including the capability to calculate eigenvalues for critical systems. For this study, the continuous-energy (CE) transport calculations of neutrons with Evaluated Nuclear Data Files (ENDF)/B-VII.0 cross section libraries and of photons with MCPLIB04 are only considered. MCNP has several inherent variance reduction technique options to accelerate the transport calculations. The analog MCNP calculations (i.e., using no variance

reduction techniques) performed in this paper are based on the parallel version of MCNP on the Y-12 cluster using a single node having 24 processors. **NOTE:** In this paper, "analog MCNP" is hereafter referred to as "MCNP."

The ADVANTG code [3] developed at ORNL automates the generation of variance reduction parameters for CE Monte Carlo simulations of fixed-source neutron, photon, and coupled neutron-photon transport problems using MCNP. ADVANTG generates space- and energy-dependent mesh-based weight-window bounds and biased source distributions from 3-D discrete ordinate (S_N) calculations that are performed by Denovo computer code [5]. The final variance reduction parameters are output in a format that can be used with an automatic modified (for the biased parameters and weight-window generators) version of a MCNP input file to accelerate the convergence process. ADVANTG implements the Consistent Adjoint Driven Importance Sampling (CADIS) method and the Forward-Weighted CADIS (FW-CADIS) method for generating variance reduction parameters. The CADIS method was developed for accelerating individual tallies, whereas, FW-CADIS can be applied to multiple tallies and mesh tallies. In this study, the FW-CADIS method in ADVANTG is used. Calculations using the parallel version of MCNP are performed with the ADVANTG-generated input file. The ENDF/B-VII.0 cross section libraries for photons and neutrons used for ADVANTG calculations are coupled 27-neutron/19-gamma (27n19g) and coupled 200-neutron/47-gamma (200n47g) group structures. ADVANTG and MCNP calculations were performed on a Y-12 cluster using multiple processors.

Monaco [4] is a general-purpose fixed source Monte Carlo shielding transport code for analyses of multidimensional neutron, photon, and coupled problems. Monaco is part of the SCALE modeling and simulation suite developed at ORNL for nuclear safety analysis and design, and uses the SCALE General Geometry Package, which is the same geometry description as KENO-VI [4]. Monaco has many options available to the user for specifying the source distributions, tally options, and variance reduction capabilities. Monaco, originally based on the obsolete MORSE Monte Carlo code, has been extensively modified to modernize the coding and increases the number of capabilities in terms of sources and tallies. Monaco in SCALE 6.1 is limited to multigroup energy transport capabilities while that in SCALE 6.2 has

the option to use CE transport through the use of the new SCALE CE Modular Physics Package. Monaco is the key component of the MAVRIC sequence and uses Denovo to create the mesh-based importance map and mesh-based biased source distribution for general 3-D automated variance reduction. The Monaco calculations, based on the analog Monaco code (i.e., using no variance reduction techniques) in SCALE 6.1.1, are performed on a cluster using a single processor at Y-12. Monaco uses the already processed AMPX cross sections to calculate neutron and photon fluxes and response to point detectors. The ENDF/B-VII.0 cross section data library used in these calculations is 200n47g. **NOTE:** In this paper, "analog Monaco" is hereafter referred to as "Monaco."

MAVRIC sequence code [4], which is part of the SCALE suite developed at ORNL for shielding analyses, is based on the CADIS and FW-CADIS methodologies [8], [9], [10]. MAVRIC automatically performs 3-D, discrete-ordinate calculations using Denovo code to compute the adjoint flux as a function of position and energy. This adjoint flux information is used to construct an importance map (i.e., target weights for weight windows) and a biased source distribution that work together; particles are born with a weight matching the target weight of the cell into which they are born. The FW-CADIS methodologies in MAVRIC are used to optimize dose rates for all detector locations in a single simulation. Monaco code uses the importance map for biasing during particle transport using the biased source distribution as its source for the Monte Carlo simulation. During transport, the particle weight is compared to the importance map after each particle interaction and whenever a particle crosses into a new importance cell in the map. For problems that do not require variance reduction to complete in a reasonable time, execution of MAVRIC without the importance map calculation provides an easy approach to run Monaco. For problems that require variance reduction to complete in a reasonable time, MAVRIC removes the burden of manually setting weight windows and performs it automatically with a minimal amount of additional input. MAVRIC sequence can be used with the final Monaco calculation as either a multigroup calculation in SCALE 6.0, 6.1, or 6.2 or as a CE calculation in SCALE 6.2. The calculations performed in this paper are based on the MAVRIC/Monaco/Denovo codes with FW-CADIS methodologies in SCALE 6.1.1 on a cluster using a single processor. The ENDF/B-VII.0 cross section data library used in these calculations is 200n47g.

The following supporting computer codes are used by MCNP, ADVANTG, Monaco, and MAVRIC:

- ORIGEN-S [4] is a general purpose point depletion and decay code. Given an initial isotopic distribution, materials are decayed to provide time-dependent, energy-grouped photon and neutron sources. ORIGEN cases were run using SCALE 6.1.1 on a Y-12 cluster.
- Denovo [4] is a 3-D block-parallel discrete ordinates transport S_N code developed at ORNL as part of SCALE. The Denovo code is used to generate adjoint scalar fluxes for the CADIS or FW-CADIS method in MAVRIC. The Denovo code is fast, positive, and robust. The phase-space shape of the forward and adjoint fluxes, as opposed to a highly accurate solution, is the most important quality for Monte Carlo weight-window generation. Denovo uses an orthogonal, nonuniform mesh that is ideal for CADIS applications because of the speed and robustness of the calculations on this mesh type. Denovo uses the highly robust GMRES (Generalized Minimum Residual) Krylov method to solve the S_N equations in each group. GMRES has been shown to be more robust and efficient than traditional source (fixed-point) iteration. The Denovo calculations driven by ADVANTG for ADVANTG/MCNP are performed on a Y-12 cluster using parallel processors. The ENDF/B-VII.0 cross section libraries for photons and neutrons used for ADVANTG in MCNP calculations are 27n19g and 200n47g. The Denovo calculations for the MAVRIC code are performed on a Y-12 cluster using a single processor using 200n47g in the ENDF/B-VII.0 cross section libraries for both photons and neutrons.

IV. SOURCE CONFIGURATIONS MODELED

Six different geometric configurations inside CV are modeled, and these configurations are solid cylinder, cylindrical hemi-shell, cylindrical shell, rectangular plate, cylindrical rod, and cylindrical segment. The models of these configuration are discussed below.

A solid HEU metal cylinder (6.35-cm radius and 15.1003-cm high) is placed either at the top or bottom of the CV. The side and bottom sections of the solid cylinder configuration are shown in Fig. 2.

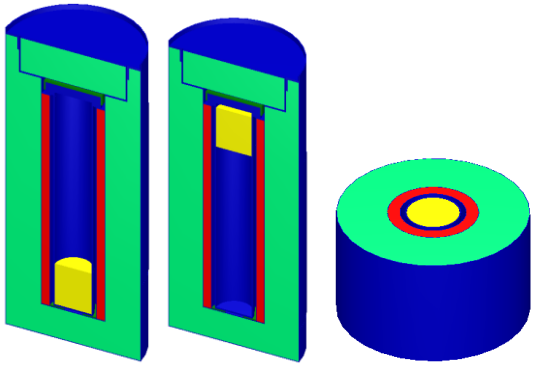

Fig. 2. Calculation model of the ES-3100 package with the solid cylinder source configuration shown in yellow (x-z side and x-y bottom sections).

A cylindrical hemi-shell (4.9337-cm inner radius, 6.35-cm outer radius, and 76.2-cm high) with the interior opening inward is placed inside the CV along the x-axis. The side and bottom sections of the cylindrical hemi-shell calculation model are shown in Fig. 3.

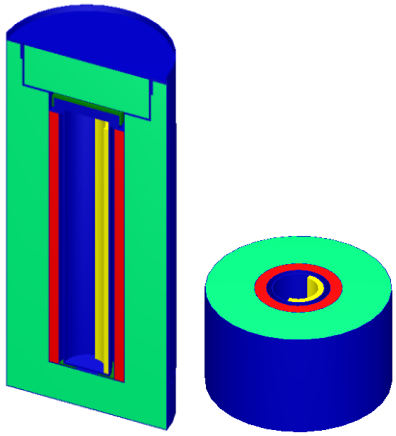

Fig. 3. Calculation model of the ES-3100 package with cylindrical hemi-shell source configuration shown in yellow (x-z side and x-y bottom sections).

A cylindrical shell (5.6861-cm inner radius, a 6.35-cm outer radius, and a 76.2-cm high) is placed inside the CV for investigating side surface dose rates. The side and bottom sections of the cylindrical shell calculation model are shown in Fig. 4.

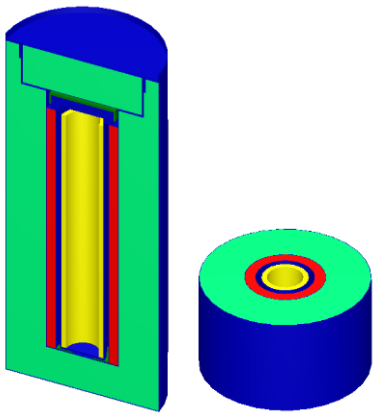

Fig. 4. Calculation model of the ES-3100 package with the cylindrical shell source configuration shown in yellow (x-z side and x-y bottom sections).

A rectangular plate (1.9829-cm wide, 12.66-cm long, and 76.2-cm high) is placed along the centerline on the y-axis. The side and bottom sections of the plate calculation model are shown in Fig. 5.

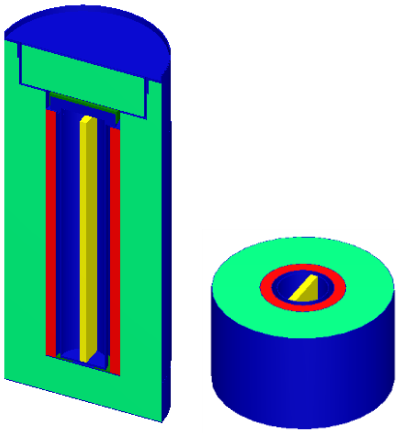

Fig. 5. Calculation model of the ES-3100 package with the plate type source configuration shown in yellow (x-z side and x-y bottom section).

A cylindrical rod (2.82675-cm radius and 76.2-cm high) is placed along the x-axis close to the CV wall. The side and bottom sections of the cylindrical rod calculation model are shown in Fig. 6.

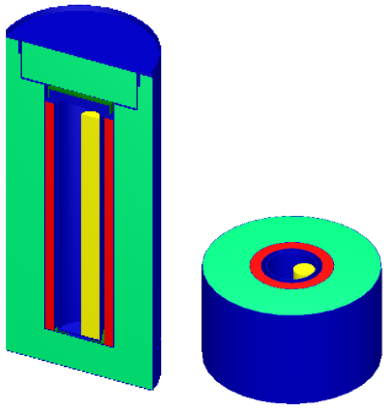

Fig. 6. Calculation model of the ES-3100 package with a single rod source configuration shown in yellow (x-z side and x-y bottom sections).

A cylindrical segment (6.35-cm radius, 76.2-cm high, 3.1442 cm from the center) is placed along the x-axis close to the CV wall. The side and bottom sections of the cylindrical segment calculation model are shown in Fig. 7.

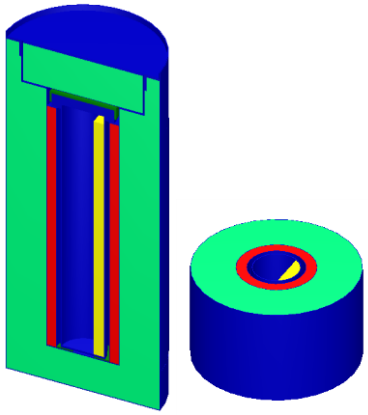

Fig. 7. Calculation model of the ES-3100 package with a cylindrical segment source configuration shown in yellow (x-z side and x-y bottom sections).

V. IMPLEMENTATION OF COMPUTATIONAL METHODS

Dose rates are calculated for different source configurations using MCNP and Monaco codes without using any of their inherent variance reduction options. In this paper, dose rates are calculated using point detector tallies for all codes. MCNP dose rate calculation convergence is accelerated using global variance reduction option FW-CADIS in ADVANTG code, which is used in MCNP to accelerate the convergence, is termed as ADVANTG/MCMP, and is discussed in Sect. V.A. Similarly, Monaco dose rate calculation convergence is accelerated in MAVRIC code, which uses FW-CADIS methods for global variance reduction and is discussed in Sect. V.B. A detailed description of the FW-CADIS method is provided in "Monte Carlo Shielding Analysis Capabilities with MAVRIC" [8].

V.A ADVANTG CALCULATIONS

ADVANTG includes a standard MCNP input file from which ADVANTG extracts the geometry of the material bodies, material compositions, fixed-source distributions, tally regions, and response spectra. ADVANTG also reads an additional input file that contains a Cartesian structure grid, parameters for the Denovo discrete ordinate calculations, and options for the CADIS and FW-CADIS calculations. The spatial mesh grid is used for the deterministic calculations and for the space- and energy-dependent weight windows that are generated by the CADIS or FW-CADIS calculation. It may be noted that the FW-CADIS method is used in this paper. ADVANTG performs a series of several steps when executing a FW-CADIS calculation. A discretized version of the Monte Carlo problem is constructed for the discrete ordinate calculation. A forward-mode Denovo calculation is executed, and the scalar flux output is used to construct an adjoint source. An adjoint-mode Denovo calculation is executed, and the resulting flux distribution is used to compute weight window lower bounds and consistent biased source distribution. The biased source distribution is generated directly on the space and energy bins that were used to describe the source in the MCNP input file. The CADIS and FW-CADIS methods creates the discretized version of the Monte Carlo problem for the discrete ordinate calculations. ADVANTG uses ray tracing to estimate material fraction in each cell. The MCNP material composition is translated into a suitable form to use with the multigroup

cross section library by the user. The variance reduction parameter output files are written as a *wwinp* file for the space- and energy-dependent weight window lower bounds and *sdef* cards for the biased source distribution that are incorporated into the user MCNP input file.

V.B MAVRIC CALCULATIONS

The SCALE code system includes the Monaco fixed-source multigroup Monte Carlo code, the Denovo Cartesian mesh discrete ordinate code, and MAVRIC sequence for using the CADIS and the FW-CADIS methods. Monaco uses the same combinatorial solid-body geometry description and multigroup cross section processing as the KENO-VI/CSAS6 criticality sequence in SCALE. Monaco has an easy-to-use and flexible block and keyword style input structure. This allows users to define distributions, response functions, and spatial meshes for specifying sources and tallies. The MAVRIC sequence reads an input very similar to that of Monaco with an additional block specifying information needed for the automated variance-reduction methods. This additional information consists of one or more adjoint sources corresponding to the tallies that the user wishes to optimize and a spatial mesh. MAVRIC constructs a mesh-based version of the geometry and uses Denovo to calculate forward and/or adjoint fluxes. The mesh-based flux estimates calculated by Denovo use either the CADIS or the FW-CADIS methods to construct space- and energy-dependent weight windows and consistent, mesh-based source biasing parameters. These biasing parameters are passed to Monaco for the Monte Carlo calculations. The tracking and tallies in the Monaco calculations use the combinational solid-body geometry, not the mesh-based geometry used in the Denovo calculations. The user original source specifications are replaced by the biased mesh-based source specifications. The spatial meshing is fine enough in the source regions such that the mesh-based versions of the sources adequately represent the true sources.

VI. RESULTS AND DISCUSSIONS

The calculated dose rates at the package surfaces and 1 m from the package surfaces using MCNP, ADVANTG/MCNP, Monaco, and MAVRIC for different source configurations in the ES-3100 package are presented in Tables I–VII. The presented dose rates are ±1σ (one sigma) uncertainty expressed as a percentage of the mean. The comparative dose rates presented in the tables are for photons, neutrons including secondary photons, and photons plus neutrons including secondary photons. The ADVANTG/MCNP, Monaco, and MAVRIC calculated dose rates are compared against the MCNP calculated dose rates. The results between analog MCNP and ADVANTG/MCNP are in good agreement for almost all cases. The number of particles simulated is about 100 times higher (1.0×10^{10} vs 1.0×10^{8}) for analog MCNP than for ADVANTG/MCNP in most cases. Hence, ADVANTG/MCNP significantly reduces the computer run time, but it involves logistic issues of setting up the ADVATG input file to generate the biased MCNP input file, run the biased MCNP input file, and also make sure that the grid geometries are set up appropriately. The Monaco and MAVRIC neutron dose rates for the solid cylinder at the bottom and top configurations are 5 to 10% higher than the MCNP neutron dose rates. But, Monaco and MAVRIC results are in good agreement in those neutron cases. In general, the Monaco simulations are for 100 times more particles and require 100 times more computer time. The neutron dose rates constitute only 2% or less of the total dose rates. It may be noted that MCNP and Monaco are two different Monte Carlo simulation codes developed by two independent organizations. Also, one grid geometry is used to generate biased source parameters for each source configuration in ADVANTG/MCNP, although each source shape is significantly different. Similarly, another grid geometry is used for each source configuration in MAVRIC.

Photon and neutron dose rate contours are generated by the Java application, Mesh File Viewer for MCNP, ADVANTG/MCNP, Monaco, and MAVRIC cases. The grid geometry used to generate dose rate contours is 2 cm apart in x-, y-, and z-directions for each source configuration in MCNP calculations. The same grid geometry is used in ADVANTG/MCNP to calculate weight windows and biased source distributions by Denovo for MCNP. The photon and neutron dose rate contours for the cylindrical hemi-shell

configuration are presented in this paper. Figure 8 shows the MCNP photon dose rate contours near the source center for the cylindrical hemi-shell (x-y plane) along with the geometry grids. Figures 9 and 10 show the MCNP photon and neutron dose rate contours (x-z plane). The ADVANTG/MCNP-generated photon and neutron dose rate contours (x-z plane) are presented in Figs. 11 and 12. The following grid geometry is used to generate mesh tally dose rate contours for Monaco and MAVRIC for each source configuration, and the grids are shown in Figs. 13 and 14. Also, the same grid geometry is used to generate importance maps for each source configuration in MAVRIC.

```
gridGeometry 1
   xLinear  5 -125  -25
   xLinear  6  -25  -11
   xLinear 22  -11   11
   xLinear  6   11   25
   xLinear  5   25  125

   yLinear  5 -125  -25
   yLinear  6  -25  -11
   yLinear 22  -11   11
   yLinear  6   11   25
   yLinear  5   25  125

   zLinear  5 -101    0
   zLinear 44    0  110
   zLinear  5  110  211
 end gridGeometry
```

The photon and neutron dose rate contours for Monaco and MAVRIC are presented in Figs. 15–18. The mesh tally contours provide an excellent visualization whether the dose rates are calculated as expected.

TABLE I
Dose rates for HEU metal solid cylinder at the bottom of CV

With reference to drum	Dose rates (mrem/h) with ±1σ uncertainty (%)				Difference between		
	MCNP	ADVANTG/ MCNP	Monaco	MAVRIC	ADVANTG/ MCNP and MCNP (%)	Monaco and MCNP (%)	MAVRIC and MCNP (%)
Side surface (photon)	51.4290 ± 0.78	50.2790 ± 2.08	51.9019 ± 0.96	53.6403 ± 1.24	−2.2	0.9	4.3
Top surface (photon)	1.1717 ± 2.22	1.1488 ± 1.97	1.1503 ± 2.27	1.0931 ± 1.27	−2.0	−1.8	−6.7
Bottom surface (photon)	80.0030 ± 0.64	80.9200 ± 2.61	83.4852 ± 2.36	82.5673 ± 0.53	1.2	4.4	3.2
1 m from side surface (photon)	1.6257 ± 0.10	1.6195 ± 0.80	1.6873 ± 0.15	1.6514 ± 0.07	−0.4	3.8	1.6
1 m from top surface (photon)	0.1665 ± 0.18	0.1653 ± 0.55	0.1713 ± 0.39	0.1537 ± 0.07	−0.8	2.9	−7.7
1 m from bottom surface (photon)	1.4337 ± 0.15	1.4282 ± 0.65	1.4876 ± 0.16	1.4804 ± 0.07	−0.4	3.8	3.3
Side surface (neutron [a])	1.1937 ± 0.27	1.2064 ± 0.73	1.2638 ± 0.78	1.2476 ± 1.57	1.1	5.9	4.5
Top surface (neutron [a])	0.0454 ± 0.56	0.0468 ± 0.80	0.0490 ± 2.21	0.0502 ± 2.22	3.0	7.8	10.5
Bottom surface (neutron [a])	2.0354 ± 0.36	2.0569 ± 0.66	2.2049 ± 2.79	2.1243 ± 1.36	1.1	8.3	4.4
1 m from side surface (neutron [a])	0.0383 ± 0.15	0.0385 ± 0.62	0.0403 ± 0.51	0.0403 ± 1.15	0.5	5.2	5.1
1 m from top surface (neutron [a])	0.0051 ± 0.15	0.0051 ± 0.63	0.0054 ± 0.51	0.0054 ± 1.16	0.5	7.3	6.9
1 m from bottom surface (neutron [a])	0.0416 ± 0.15	0.0419 ± 0.62	0.0438 ± 0.51	0.0437 ± 1.15	0.6	5.3	4.9
Side surface (photon + neuron [a])	52.6227 ± 0.76	51.4854 ± 2.03	53.1657 ± 0.94	54.8879 ± 1.21	−2.2	1.0	4.3
Top surface (photon + neuron [a])	1.2171 ± 2.14	1.1956 ± 1.89	1.1993 ± 2.18	1.1433 ± 1.22	−1.8	−1.5	−6.1
Bottom surface (photon + neuron [a])	82.0384 ± 0.62	82.9769 ± 2.55	85.6901 ± 0.62	84.6916 ± 0.52	1.1	4.5	3.2
1 m from side surface (photon + neuron [a])	1.6640 ± 0.10	1.6580 ± 0.78	1.7276 ± 0.15	1.6917 ± 0.07	−0.4	3.8	1.7
1 m from top surface (photon + neuron [a])	0.1716 ± 0.17	1.1703 ± 0.53	0.1767 ± 0.38	0.1592 ± 0.08	−0.7	3.0	−7.2
1 m from bottom surface (photon + neuron [a])	1.4753 ± 0.15	1.4701 ± 0.63	1.5314 ± 0.16	1.5241 ± 0.08	−0.4	3.8	3.3

[a] Neutron includes secondary photon.

TABLE II
Dose rates for HEU metal solid cylinder at the top of CV

With reference to drum	Dose rates (mrem/h) with ±1σ uncertainty (%)				Difference between		
	MCNP	ADVANTG/ MCNP	Monaco	MAVRIC	ADVANTG/ MCNP and MCNP (%)	Monaco and MCNP (%)	MAVRIC and MCNP (%)
Side surface (photon)	50.6430 ± 0.59	51.2040 ± 1.33	52.3385 ± 1.06	52.4354 ± 0.87	1.1	3.4	3.5
Top surface (photon)	19.7480 ± 0.96	19.8550 ± 1.28	20.8742 ± 4.50	19.5786 ± 0.73	0.5	5.7	−0.9
Bottom surface (photon)	3.1690 ± 1.5	3.3062 ± 2.06	3.0875 ± 1.45	3.3729 ± 2.35	4.3	−2.6	6.4
1 m from side surface (photon)	1.6216 ± 0.09	1.6243 ± 0.29	1.6847 ± 0.12	1.6810 ± 0.09	0.2	3.9	3.7
1 m from top surface (photon)	0.6392 ± 0.13	0.6384 ± 0.30	0.6649 ± 0.21	0.6492 ± 0.14	−0.1	4.0	1.6
1 m from bottom surface (photon)	0.4228 ± 0.28	0.4215 ± 0.15	0.4325 ± 0.18	0.4295 ± 0.04	−0.3	2.3	1.6
Side surface (neutron [a])	1.3553 ± 0.38	1.3543 ± 2.26	1.4581 ± 0.70	1.4708 ± 1.21	−0.1	7.6	8.5
Top surface (neutron [a])	0.9376 ± 0.44	0.9537 ± 2.48	1.0139 ± 0.61	1.0268 ± 1.15	1.7	8.1	9.5
Bottom surface (neutron [a])	0.1087 ± 1.52	0.1082 ± 2.21	0.1211 ± 0.38	0.1174 ± 1.12	−0.5	11.4	8.0
1 m from side surface (neutron [a])	0.0439 ± 0.18	0.0441 ± 2.12	0.0473 ± 0.37	0.0477 ± 0.78	0.5	7.7	8.6
1 m from top surface (neutron [a])	0.0295 ± 0.18	0.0296 ± 2.17	0.0320 ± 0.37	0.0322 ± 0.81	0.4	8.4	9.1
1 m from bottom surface (neutron [a])	0.0118 ± 0.18	0.0119 ± 2.07	0.0128 ± 0.37	0.0129 ± 0.77	1.1	8.6	9.6
Side surface (photon + neuron [a])	51.9983 ± 0.37	52.5583 ± 2.25	53.7966 ± 1.03	53.9062 ± 0.85	1.1	3.5	3.7
Top surface (photon + neuron [a])	20.6856 ± 0.44	20.8087 ± 2.46	21.8881 ± 4.29	20.6054 ± 0.70	0.6	5.8	−0.4
Bottom surface (photon + neuron [a])	3.2777 ± 1.51	3.4144 ± 2.20	3.2085 ± 1.40	3.4903 ± 2.27	4.2	−2.1	6.5
1 m from side surface (photon + neuron [a])	1.6655 ± 0.18	1.6684 ± 2.10	1.7320 ± 0.12	1.7287 ± 0.09	0.2	4.0	3.8
1 m from top surface (photon + neuron [a])	0.6687 ± 0.18	0.6680 ± 2.16	0.6968 ± 0.20	0.6814 ± 0.14	−0.1	4.2	1.9
1 m from bottom surface (photon + neuron [a])	0.4345 ± 0.18	0.4334 ± 2.06	0.4453 ± 0.18	0.4424 ± 0.04	−0.3	2.5	1.8

[a] Neutron includes secondary photon.

TABLE III
Dose rates for the HEU metal cylindrical hemi-shell configuration

With reference to drum	Dose rates (mrem/h) with ±1σ uncertainty (%)				Difference between		
	MCNP	ADVANTG/ MCNP	Monaco	MAVRIC	ADVANTG/ MCNP and MCNP (%)	Monaco and MCNP (%)	MAVRIC and MCNP (%)
Side surface (photon)	95.8000 ± 1.47	95.1200 ± 1.12	97.6942 ± 1.96	100.5490±1.78	−0.7	2.0	5.0
Top surface (photon)	9.3716 ± 0.71	9.7339 ± 3.89	9.8994 ± 2.69	9.2099 ± 2.46	3.9	5.6	−1.7
Bottom surface (photon)	41.1910 ± 0.80	43.0490 ± 3.25	43.7977 ± 4.97	41.9378 ± 0.71	4.5	6.3	1.8
1 m from side surface (photon)	6.0639 ± 0.06	6.0799 ± 0.31	6.2821 ± 0.08	6.2785 ± 0.07	0.3	3.6	3.5
1 m from top surface (photon)	0.3821 ± 0.43	0.3827 ± 0.35	0.4021 ± 0.33	0.3842 ± 0.16	0.1	5.2	0.6
1 m from bottom surface (photon)	0.8479 ± 0.13	0.8507 ± 0.03	0.8861 ± 0.21	0.8733 ± 0.11	0.3	4.5	3.0
Side surface (neutron [a])	0.1335 ± 0.38	0.1334 ± 0.91	0.1343 ± 1.02	0.1334 ± 0.91	−0.1	0.6	−0.1
Top surface (neutron [a])	0.0339 ± 0.55	0.0328 ± 0.68	0.0332 ± 1.20	0.0328 ± 0.68	−3.2	−1.8	−3.2
Bottom surface (neutron [a])	0.0817 ± 0.43	0.0821 ± 1.24	0.0811 ± 0.85	0.0821 ± 1.24	0.5	−0.8	0.5
1 m from side surface (neutron [a])	0.0073 ± 0.02	0.0073 ± 0.07	0.0073 ± 0.04	0.0073 ± 0.07	0.3	0.2	0.3
1 m from top surface (neutron [a])	0.0013 ± 0.04	0.0012 ± 0.13	0.0013 ± 0.09	0.0012 ± 0.13	−0.6	0.4	−0.6
1 m from bottom surface (neutron [a])	0.0019 ± 0.03	0.0019 ± 0.08	0.0019 ± 0.07	0.0019 ± 0.08	−0.5	−0.2	−0.5
Side surface (photon + neuron [a])	95.9335 ± 1.47	95.2536 ± 1.12	97.8285 ± 1.96	100.6824±1.78	−0.7	2.0	5.0
Top surface (photon + neuron [a])	9.4055 ± 0.71	9.7667 ± 3.88	9.9326 ± 2.68	9.2427 ± 2.45	3.8	5.6	−1.7
Bottom surface (photon + neuron [a])	41.2727 ± 0.80	43.1311 ± 3.24	43.8788 ± 4.96	42.0199 ± 0.71	4.5	6.3	1.8
1 m from side surface (photon + neuron [a])	6.0712 ± 0.06	6.0872 ± 0.31	6.2894 ± 0.08	6.2858 ± 0.07	0.3	3.6	3.5
1 m from top surface (photon + neuron [a])	0.3834 ± 0.43	0.3839 ± 0.35	0.4034 ± 0.33	0.3855 ± 0.16	0.1	5.2	0.5
1 m from bottom surface (photon + neuron [a])	0.8498 ± 0.13	0.8526 ± 0.30	0.8880 ± 0.21	0.8752 ± 0.11	0.3	4.5	3.0

[a] Neutron includes secondary photon.

TABLE IV
Dose rates for the HEU metal cylindrical shell configuration

With reference to drum	Dose rates (mrem/h) with ±1σ uncertainty (%)				Difference between		
	MCNP	ADVANTG/ MCNP	Monaco	MAVRIC	ADVANTG/ MCNP and MCNP (%)	Monaco and MCNP (%)	MAVRIC and MCNP (%)
Side surface (photon)	94.5910 ± 2.24	93.1490 ± 2.82	96.2282 ± 1.01	94.3998 ± 0.69	−1.5	1.7	−0.2
Top surface (photon)	16.5450 ± 2.04	16.3870 ± 3.34	17.6263 ± 4.55	17.4100 ± 3.62	−1.0	6.5	5.2
Bottom surface (photon)	72.3600 ± 1.35	72.4850 ± 2.22	74.7124 ± 1.33	74.4352 ± 0.80	0.2	3.3	4.3
1 m from side surface (photon)	6.0043 ± 0.05	6.0186 ± 0.34	6.2356 ± 0.02	6.1656 ± 0.05	0.2	3.9	2.7
1 m from top surface (photon)	0.5662 ± 0.25	0.5641 ± 0.63	0.5912 ± 0.09	0.5945 ± 0.12	−0.4	4.4	5.0
1 m from bottom surface (photon)	1.2692 ± 0.07	1.2677 ± 0.36	1.3298 ± 0.05	1.3491 ± 0.08	−0.1	4.8	6.3
Side surface (neutron [a])	0.1039 ± 1.07	0.1046 ± 1.03	0.1034 ± 0.43	0.1021 ± 0.75	0.7	−0.5	−1.8
Top surface (neutron [a])	0.0363 ± 1.43	0.0364 ± 0.80	0.0374 ± 1.13	0.0364 ± 0.97	0.1	2.9	0.1
Bottom surface (neutron [a])	0.0881 ± 0.86	0.0891 ± 0.51	0.0895 ± 0.63	0.0908 ± 1.37	1.2	1.7	3.0
1 m from side surface (neutron [a])	0.0060 ± 0.05	0.0060 ± 0.13	0.0060 ± 0.02	0.0060 ± 0.08	−0.1	0.0	−0.0
1 m from top surface (neutron [a])	0.0013 ± 0.08	0.0013 ± 0.25	0.0013 ± 0.05	0.0013 ± 0.15	−0.2	0.3	0.1
1 m from bottom surface (neutron [a])	0.0021 ± 0.08	0.0021 ± 0.15	0.0021 ± 0.04	0.0021 ± 0.09	0.0	0.0	0.6
Side surface (photon + neuron [a])	94.6949 ± 2.24	93.2536 ± 2.82	96.3316 ± 1.01	94.5019 ± 0.69	−1.5	1.7	−0.2
Top surface (photon + neuron [a])	16.5813 ± 2.04	16.4234 ± 3.33	17.6637 ± 4.54	17.4464 ± 3.61	−1.0	6.5	5.2
Bottom surface (photon + neuron [a])	72.4481 ± 1.35	72.5741 ± 2.22	74.8019 ± 1.33	75.5260 ± 0.80	0.2	3.3	4.3
1 m from side surface (photon + neuron [a])	6.0103 ± 0.05	6.0246 ± 0.34	6.2416 ± 0.02	6.1716 ± 0.05	0.2	3.9	2.7
1 m from top surface (photon + neuron [a])	0.5675 ± 0.25	0.5654 ± 0.63	0.5926 ± 0.09	0.5959 ± 0.12	−0.4	4.4	5.0
1 m from bottom surface (photon + neuron [a])	1.2713 ± 0.07	1.2698 ± 0.36	1.3319 ± 0.05	1.3512 ± 0.08	−0.1	4.8	6.3

[a] Neutron includes secondary photon.

TABLE V
Dose rates for the HEU metal rectangular plate configuration

With reference to drum	Dose rates (mrem/h) with ±1σ uncertainty (%)				Difference between		
	MCNP	ADVANTG/ MCNP	Monaco	MAVRIC	ADVANTG/ MCNP and MCNP (%)	Monaco and MCNP (%)	MAVRIC and MCNP (%)
Side surface (photon)	91.6170 ± 1.50	89.9690 ± 1.71	97.6333 ± 3.09	94.2311 ± 1.21	−1.8	6.6	2.9
Top surface (photon)	5.9658 ± 1.28	5.9594 ± 1.73	6.0086 ± 1.95	6.0079 ± 1.92	−0.1	0.7	0.7
Bottom surface (photon)	24.3270 ± 1.21	24.3080 ± 1.13	24.6337 ± 2.12	25.3950 ± 0.93	−0.1	1.3	4.4
1 m from side surface (photon)	5.8423 ± 0.05	5.8233 ± 0.31	6.0517 ± 1.95	6.0596 ± 0.05	−0.3	3.6	3.7
1 m from top surface (photon)	0.3089 ± 0.36	0.3091 ± 0.75	0.3235 ± 0.38	0.3149 ± 0.23	0.1	4.7	1.9
1 m from bottom surface (photon)	0.6639 ± 0.13	0.6667 ± 0.55	0.7016 ± 0.24	0.7056 ± 0.16	0.4	5.7	6.3
Side surface (neutron [a])	0.1214 ± 1.84	0.1217 ± 0.87	0.1238 ± 1.22	0.1252 ± 2.88	0.2	2.0	3.2
Top surface (neutron [a])	0.0295 ± 3.14	0.0290 ± 1.23	0.0282 ± 1.04	0.0295 ± 3.68	−1.7	−4.4	−0.1
Bottom surface (neutron [a])	0.0623 ± 1.62	0.0621 ± 0.61	0.0615 ± 0.94	0.0610 ± 0.95	−0.3	−1.3	−2.0
1 m from side surface (neutron [a])	0.0071 ± 0.05	0.0071 ± 0.16	0.0072 ± 0.04	0.0072 ± 0.09	−0.2	0.5	0.2
1 m from top surface (neutron [a])	0.0012 ± 0.11	0.0012 ± 0.30	0.0012 ± 0.09	0.0012 ± 0.18	0.1	0.3	−0.8
1 m from bottom surface (neutron [a])	0.0018 ± 0.09	0.0018 ± 0.17	0.0017 ± 0.08	0.0017 ± 0.11	−0.2	−0.5	−0.8
Side surface (photon + neuron [a])	91.7384 ± 1.50	90.0907 ± 1.71	97.7571 ± 3.09	94.3563 ± 1.21	−1.8	6.6	2.9
Top surface (photon + neuron [a])	5.9953 ± 1.27	5.9884 ± 1.72	6.0368 ± 1.94	6.0374 ± 1.91	−0.1	0.7	0.7
Bottom surface (photon + neuron [a])	24.3893 ± 1.21	24.3701 ± 1.13	24.6952 ± 2.11	25.4560 ± 0.93	−0.1	1.3	4.4
1 m from side surface (photon + neuron [a])	5.8494 ± 0.05	5.8304 ± 0.31	6.0588 ± 1.95	6.0667 ± 0.05	−0.3	3.6	3.7
1 m from top surface (photon + neuron [a])	0.3101 ± 0.36	0.3102 ± 0.75	0.3247 ± 0.38	0.3161 ± 0.23	0.1	4.7	1.9
1 m from bottom surface (photon + neuron [a])	0.6656 ± 0.13	0.6684 ± 0.55	0.7033 ± 0.24	0.7073 ± 0.16	0.4	5.7	6.3

[a] Neutron includes secondary photon.

TABLE VI
Dose rates for the HEU metal cylindrical rod configuration

With reference to drum	Dose rates (mrem/h) with ±1σ uncertainty (%)				Difference between		
	MCNP	ADVANTG/ MCNP	Monaco	MAVRIC	ADVANTG/ MCNP and MCNP (%)	Monaco and MCNP (%)	MAVRIC and MCNP (%)
Side surface (photon)	58.7820 ± 0.46	58.7110 ± 1.2	61.9928 ± 2.34	61.4140 ± 0.91	−0.1	5.5	4.5
Top surface (photon)	5.1016 ± 2.84	5.0950 ± 3.75	4.7910 ± 1.60	4.7151 ± 2.13	−0.1	−6.1	−7.6
Bottom surface (photon)	20.4820 ± 1.15	20.3090 ± 1.36	21.1370 ± 4.21	21.5160 ± 0.83	−0.8	3.2	5.1
1 m from side surface (photon)	3.5115 ± 0.07	3.5061 ± 0.32	3.6374 ± 0.10	3.6010 ± 0.07	−0.2	3.6	2.6
1 m from top surface (photon)	0.2268 ± 0.15	0.2269 ± 0.71	0.2391 ± 0.43	0.2260 ± 0.17	0.0	5.4	−0.3
1 m from bottom surface (photon)	0.4966 ± 0.10	0.4971 ± 0.5	0.5220 ± 0.27	0.5180 ± 0.11	0.1	5.1	4.3
Side surface (neutron [a])	0.1635 ± 0.79	0.1643 ± 1.82	0.1623 ± 0.53	0.1623 ± 0.59	0.5	−0.7	−0.7
Top surface (neutron [a])	0.0316 ± 1.29	0.0290 ± 2.28	0.0313 ± 1.05	0.0307 ± 1.85	−8.2	−0.9	−2.9
Bottom surface (neutron [a])	0.0725 ± 1.20	0.0714 ± 0.21	0.0720 ± 0.99	0.0685 ± 1.17	−1.6	−0.8	−5.6
1 m from side surface (neutron [a])	0.0086 ± 0.05	0.0086 ± 0.22	0.0086 ± 0.04	0.0086 ± 0.10	−0.1	0.3	0.2
1 m from top surface (neutron [a])	0.0013 ± 0.11	0.0013 ± 0.83	0.0013 ± 0.10	0.0013 ± 0.29	−0.8	0.5	−0.7
1 m from bottom surface (neutron [a])	0.0020 ± 0.10	0.0020 ± 0.10	0.0020 ± 0.08	0.0020 ± 0.25	−0.1	−0.4	−0.4
Side surface (photon + neuron [a])	58.9455 ± 0.46	58.8753 ± 1.20	62.1551 ± 2.33	61.5763 ± 0.91	−0.1	5.5	4.5
Top surface (photon + neuron [a])	5.1332 ± 2.82	5.1240 ± 3.73	4.8223 ± 1.59	4.7457 ± 2.12	−0.2	−6.1	−7.6
Bottom surface (photon + neuron [a])	20.5545 ± 1.15	20.3804 ± 1.36	21.2090 ± 4.20	21.4845 ± 0.83	−0.9	3.2	4.5
1 m from side surface (photon + neuron [a])	3.5201 ± 0.07	3.5147 ± 0.32	3.6460 ± 0.10	3.6096 ± 0.07	−0.2	3.6	2.5
1 m from top surface (photon + neuron [a])	0.2281 ± 0.15	0.2282 ± 0.71	0.2404 ± 0.43	0.2273 ± 0.17	0.0	5.4	−0.4
1 m from bottom surface (photon + neuron [a])	0.4986 ± 0.10	0.4992 ± 0.55	0.5240 ± 0.27	0.5200 ± 0.11	0.1	5.1	4.3

[a] Neutron includes secondary photon.

TABLE VII
Dose rates for the HEU metal cylindrical segment configuration

With reference to drum	Dose rates (mrem/h) with ±1σ uncertainty (%)				Difference between		
	MCNP	ADVANTG MCNP	Monaco	MAVRIC	ADVANTG/ MCNP and MCNP (%)	Monaco and MCNP (%)	MAVRIC and MCNP (%)
Side surface (photon)	94.3050 ± 1.19	92.4010 ± 1.68	96.6086 ± 0.93	100.3910±1.89	−2.0	2.4	6.5
Top surface (photon)	6.7257 ± 1.78	6.6582 ± 2.54	7.2332 ± 3.78	6.3327 ± 1.31	−1.0	7.6	−5.8
Bottom surface (photon)	28.6270 ± 1.41	28.2940 ± 3.05	28.2703 ± 1.02	28.3409 ± 0.74	−1.2	−1.3	−1.0
1 m from side surface (photon)	5.5070 ± 0.05	5.4882 ± 0.36	5.7042 ± 0.06	5.7388 ± 0.07	−0.3	3.6	4.2
1 m from top surface (photon)	0.2853 ± 0.20	0.2863 ± 0.76	0.3006 ± 0.29	0.2822 ± 0.17	0.4	5.4	−1.1
1 m from bottom surface (photon)	0.6320 ± 0.09	0.6257 ± 0.43	0.6643 ± 0.18	0.6482 ± 0.11	−1.0	5.1	2.6
Side surface (neutron [a])	0.1757 ± 1.74	0.1717 ± 0.63	0.1735 ± 0.65	0.1824 ± 3.04	−2.26	−1.3	3.8
Top surface (neutron [a])	0.0322 ± 1.06	0.0325 ± 1.31	0.0319 ± 0.68	0.0347 ± 9.84	1.1	−0.9	8.1
Bottom surface (neutron [a])	0.0764 ± 1.20	0.0757 ± 0.56	0.0749 ± 0.76	0.0766 ± 0.90	−0.9	−1.9	0.2
1 m from side surface (neutron [a])	0.0089 ± 0.05	0.0089 ± 0.17	0.0089 ± 0.04	0.0089 ± 0.08	−0.0	0.4	0.8
1 m from top surface (neutron [a])	0.0013 ± 0.11	0.0013 ± 0.32	0.0013 ± 0.09	0.0013 ± 0.18	0.0	0.4	−0.9
1 m from bottom surface (neutron [a])	0.0020 ± 0.09	0.0020 ± 0.19	0.0020 ± 0.08	0.0020 ± 0.10	0.1	−0.3	0.2
Side surface (photon + neuron [a])	94.4807 ± 1.19	92.5727 ± 1.68	96.7821 ± 0.93	100.5734±1.89	−2.0	2.5	6.5
Top surface (photon + neuron [a])	6.7579 ± 1.77	6.6907 ± 2.53	7.2650 ± 3.76	6.3675 ± 1.30	−1.0	7.5	−5.8
Bottom surface (photon + neuron [a])	28.7034 ± 1.41	28.3697 ± 3.04	28.3452 ± 1.02	28.4175 ± 0.74	−1.2	−1.3	−1.0
1 m from side surface (photon + neuron [a])	5.5159 ± 0.05	5.4971 ± 0.36	5.7131 ± 0.06	5.7478 ± 0.07	−0.3	3.6	4.2
1 m from top surface (photon + neuron [a])	0.2866 ± 0.20	0.2876 ± 0.76	0.3019 ± 0.29	0.2834 ± 0.17	0.4	5.4	−1.1
1 m from bottom surface (photon + neuron [a])	0.6339 ± 0.09	0.6277 ± 0.43	0.6662 ± 0.18	0.6501 ± 0.11	−1.0	5.1	2.6

[a] Neutron includes secondary photon.

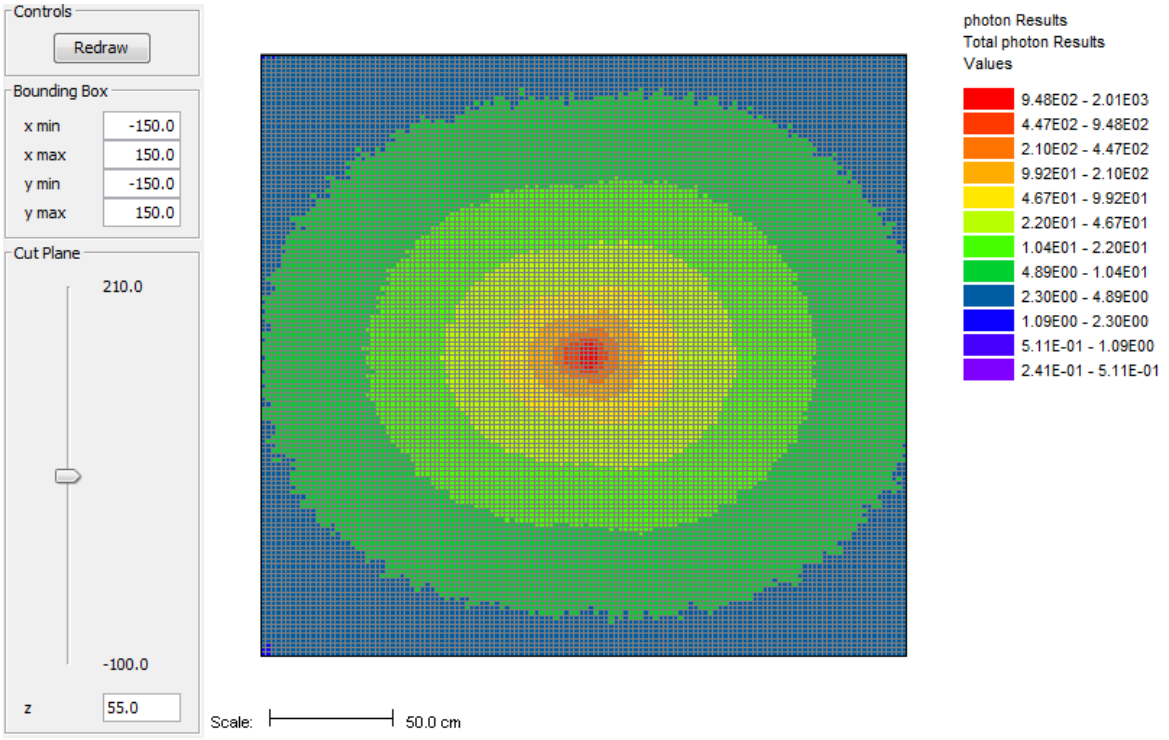

Fig. 8. MCNP photon dose rate contours near the source center for the cylindrical hemi-shell of the CV configuration (x-y plane) with mesh tally grids shown.

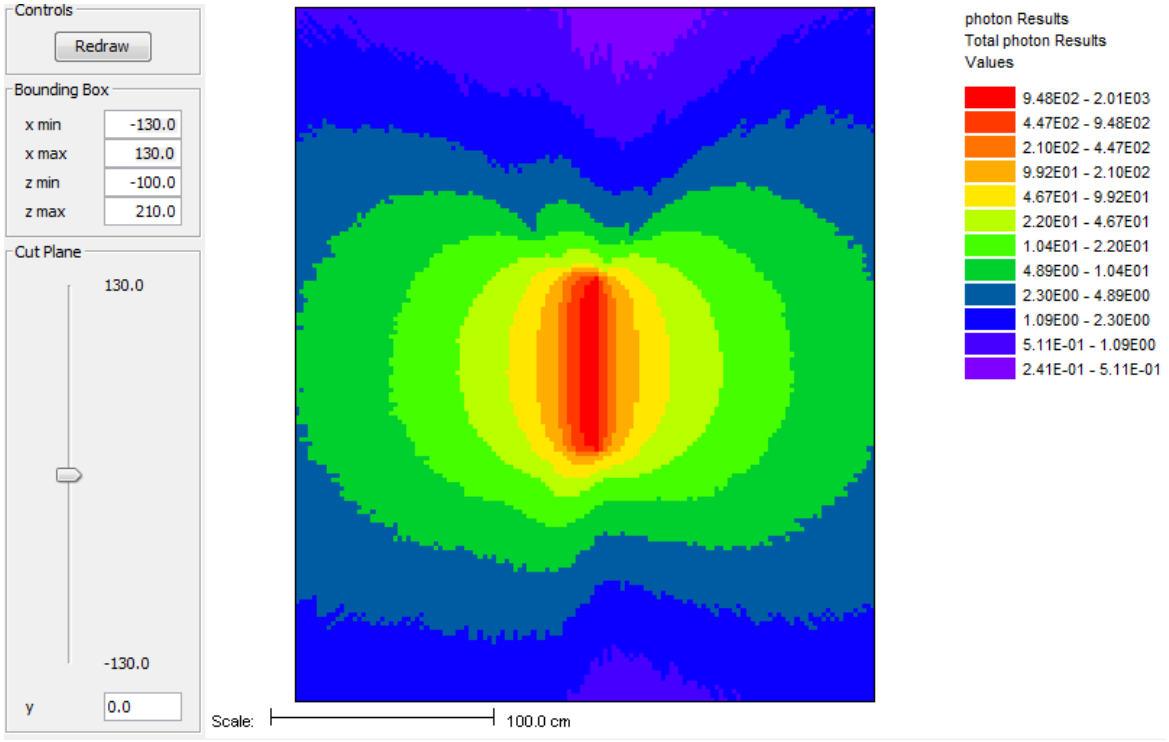

Fig. 9. MCNP photon dose rate contours for the cylindrical hemi-shell at the bottom of the CV configuration (x-z plane).

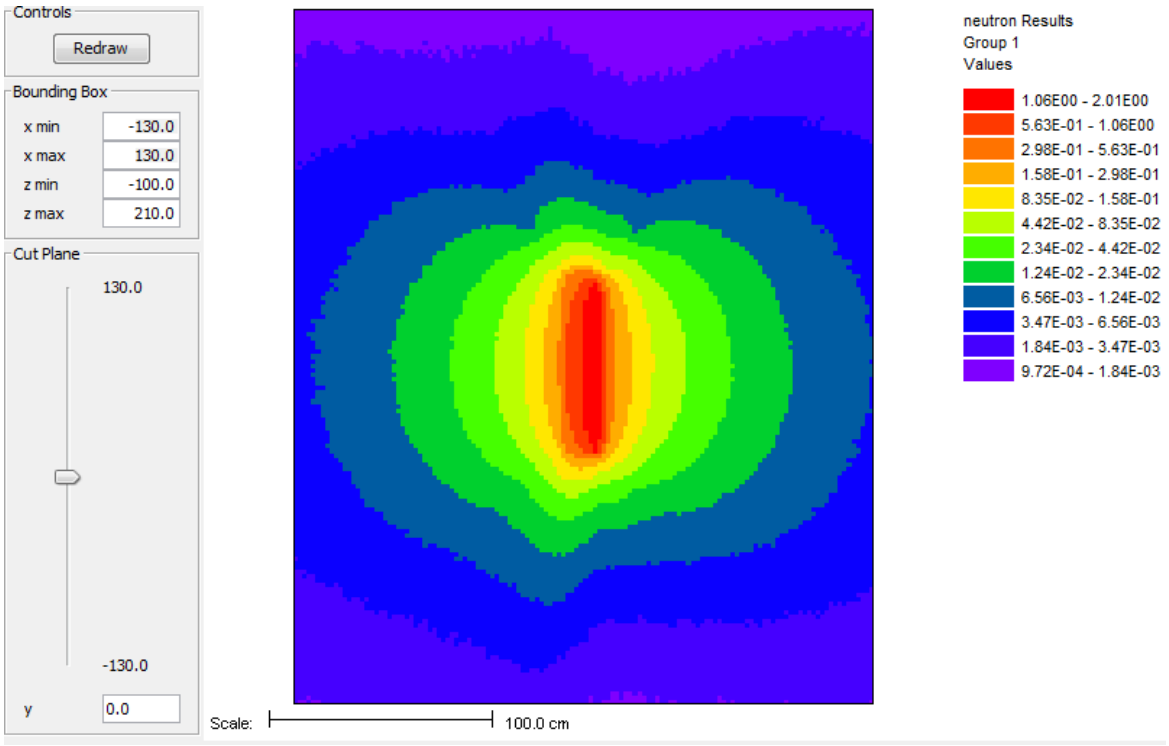

Fig. 10. MCNP neutron dose rate contours for the cylindrical hemi-shell at the bottom of the CV configuration (x-z plane).

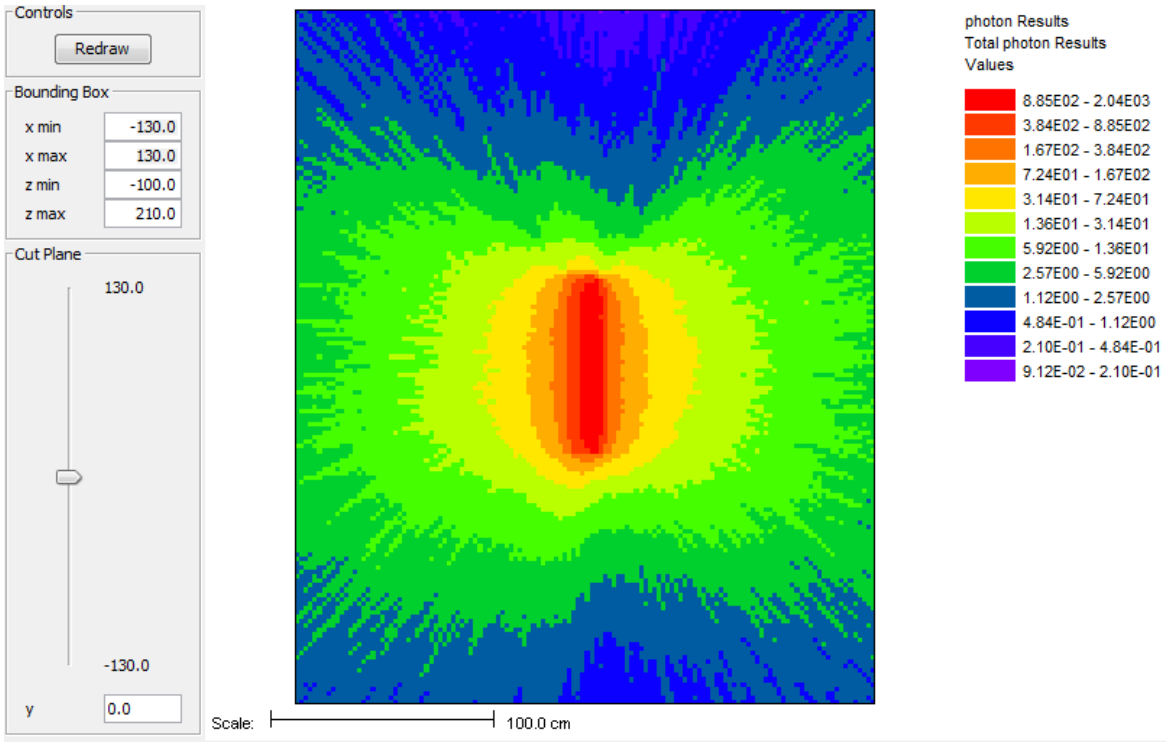

Fig. 11. ADVANTG/MCNP-generated photon dose rate contours for the cylindrical hemi-shell configuration (x-z plane).

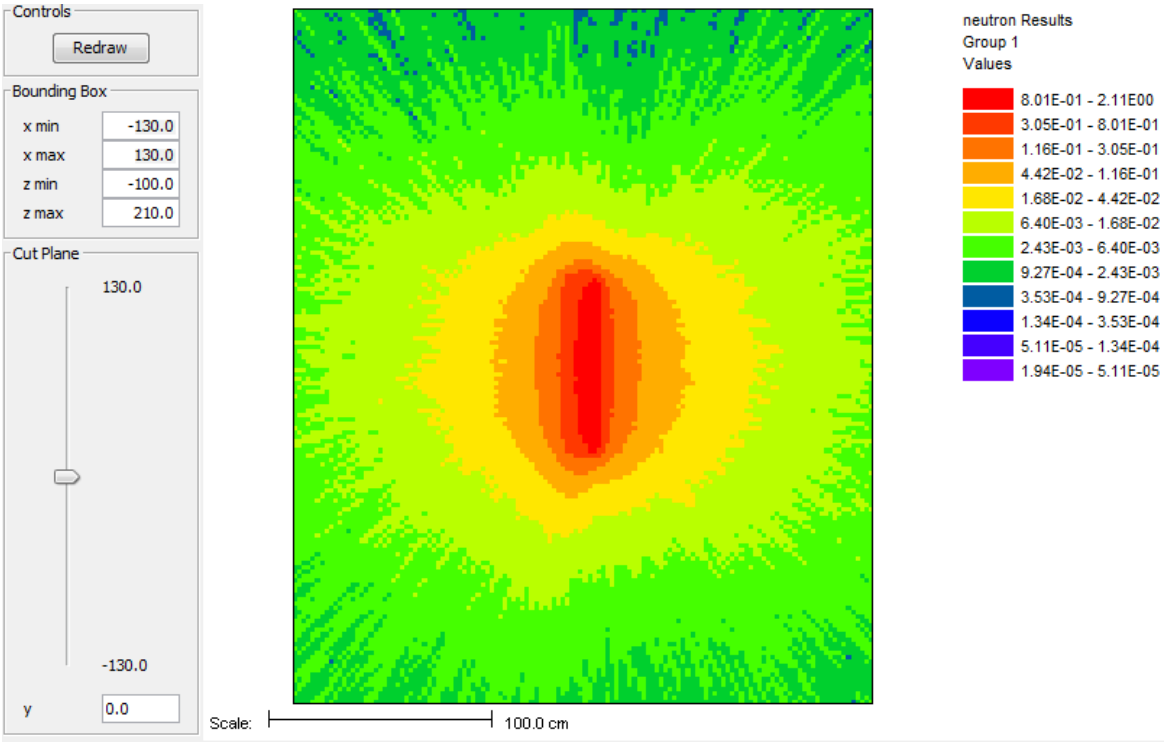

Fig. 12. ADVANTG/MCNP-generated neutron dose rate contours for the cylindrical hemi-shell configuration (x-z plane).

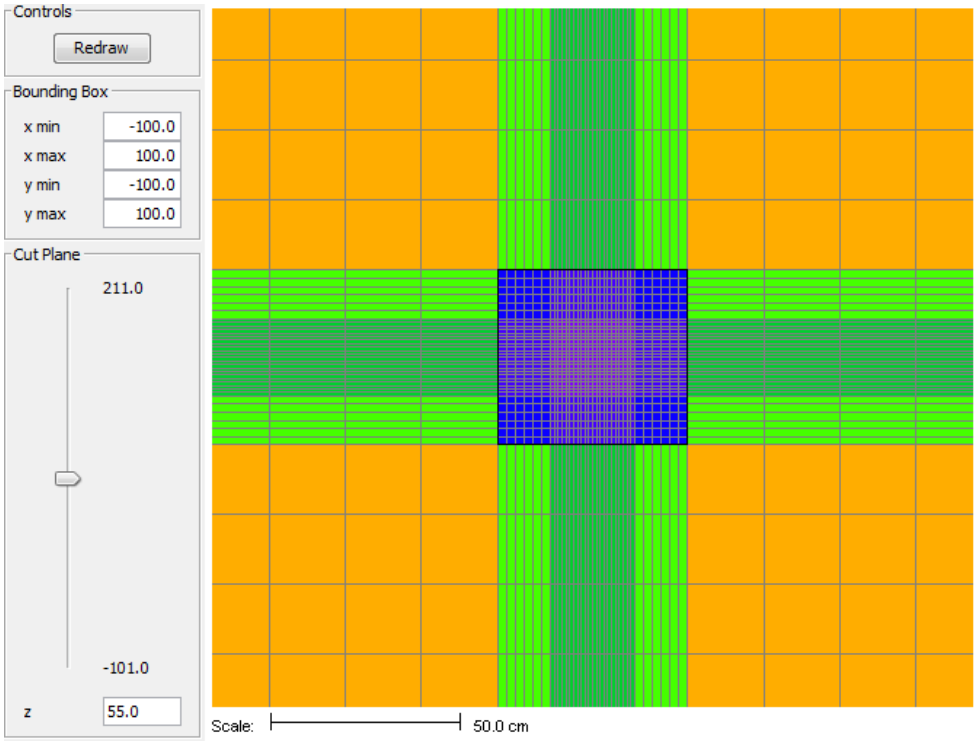

Fig. 13. Mesh grid (x-y plane) used in Monaco and MAVRIC to generate dose rate contours.

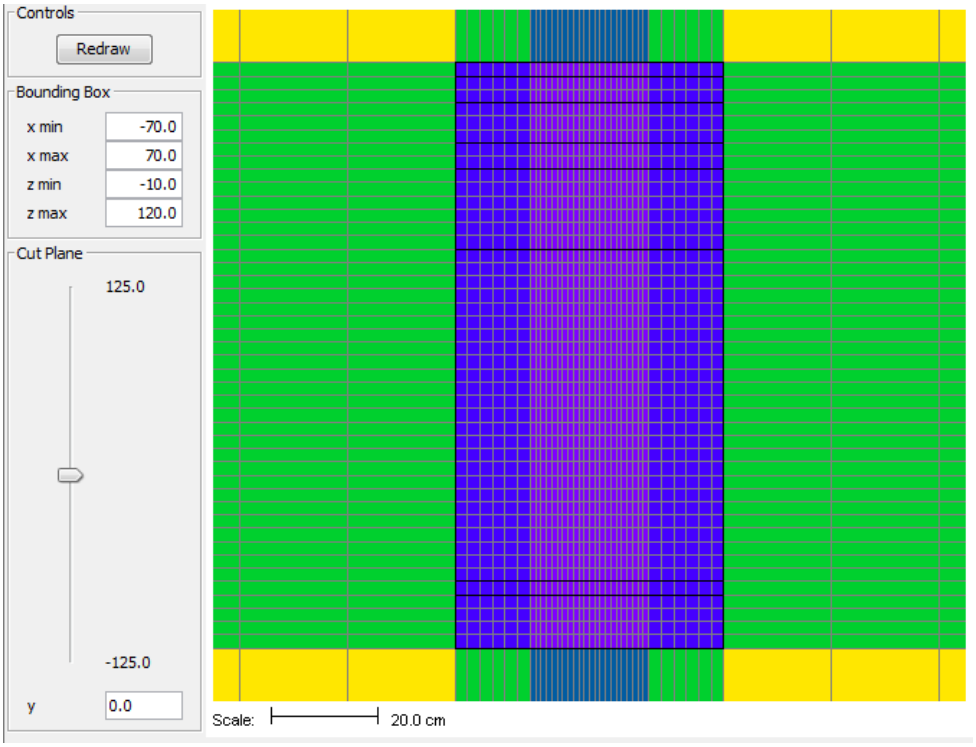

Fig. 14. Mesh grid (x-y plane) used in Monaco and MAVRIC to generate dose rate contours.

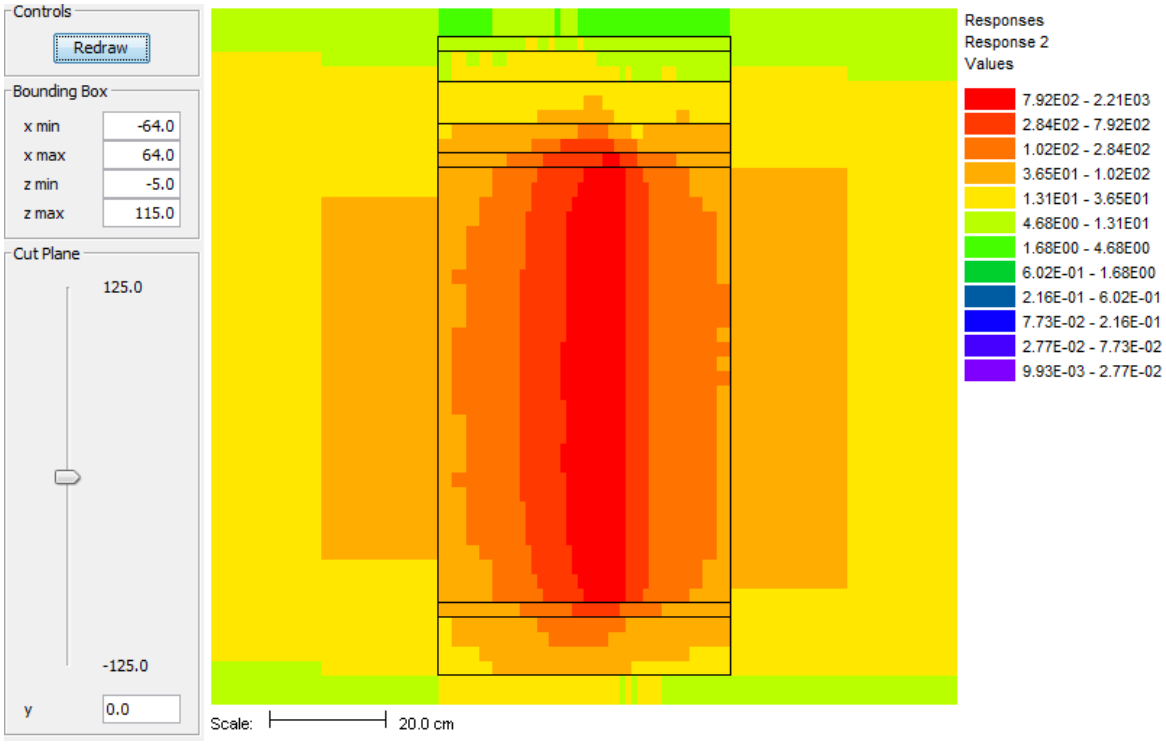

Fig. 15. Monaco-generated photon dose rate contours for the cylindrical hemi-shell configuration (x-z plane).

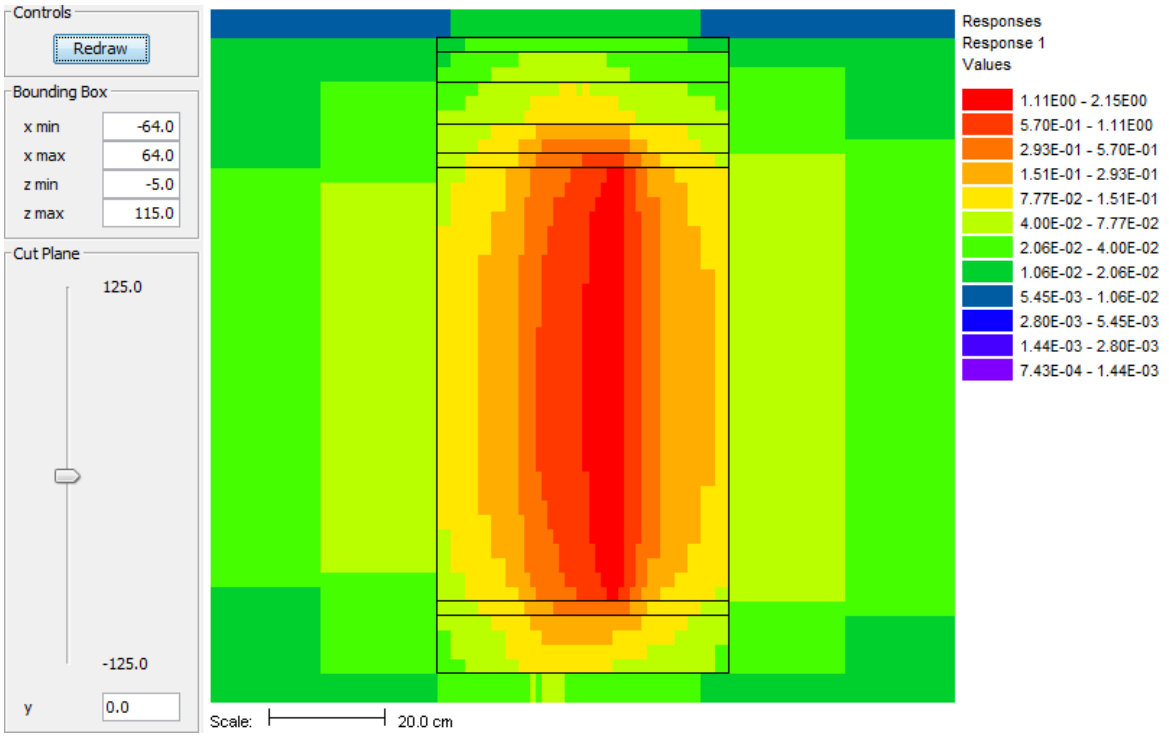

Fig. 16. Monaco-generated neutron dose rate contours for the cylindrical hemi-shell configuration (x-z plane).

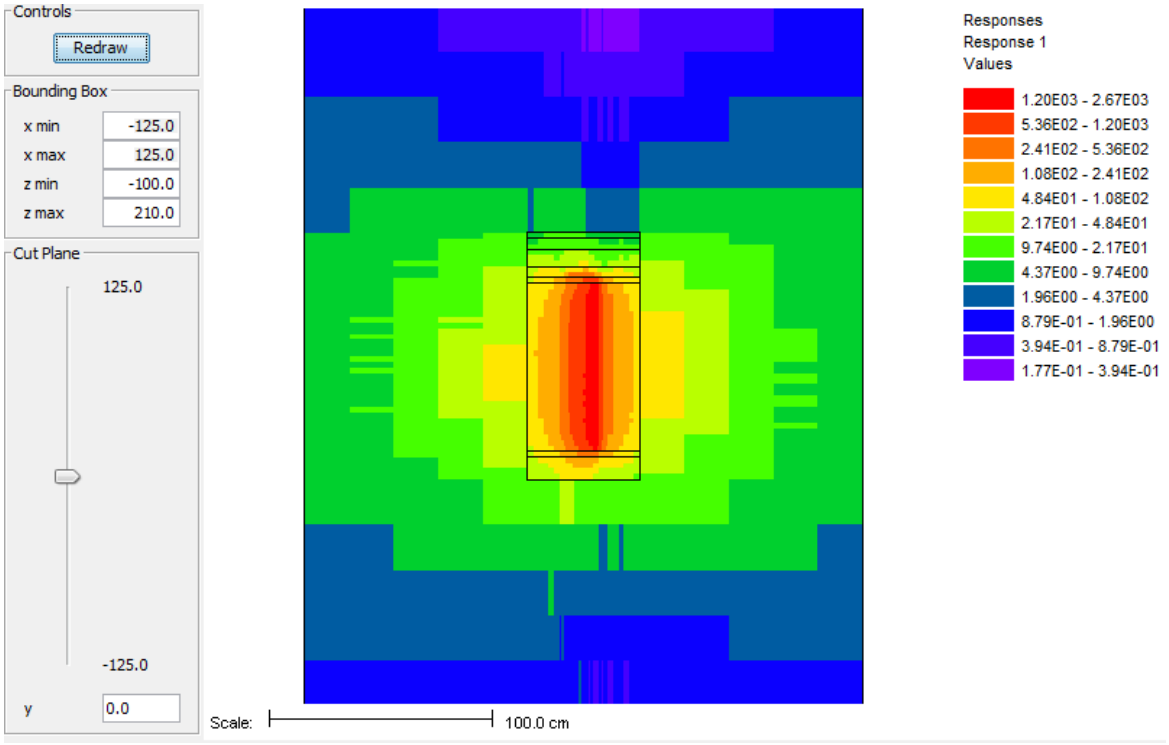

Fig. 17. MAVRIC photon dose rate contours for the cylindrical hemi-shell configuration (x-z plane).

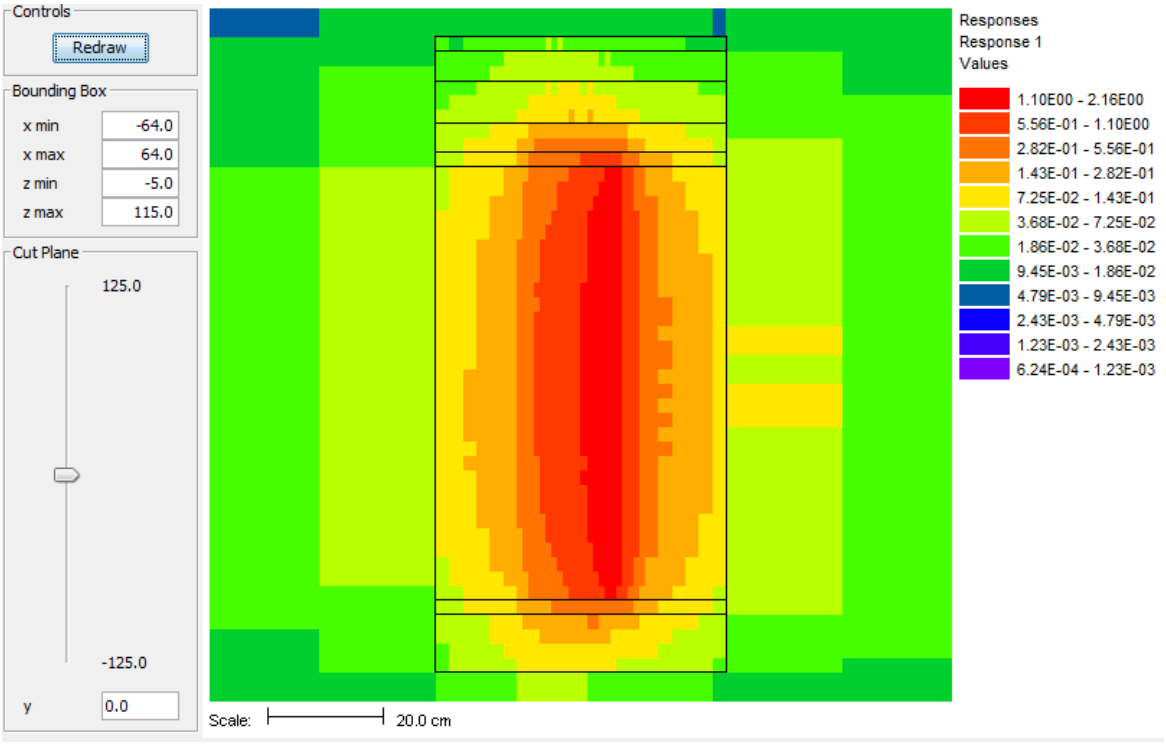

Fig. 18. MAVRIC neutron dose rate contours for the cylindrical hemi-shell configuration (x-z plane).

VII. CONCLUSIONS

The MCNP, ADVANTG/MCNP, Monaco, and MAVRIC codes produced reasonable agreement results for different source configurations evaluated in this study. If the variance reduction code (ADVANTG/MCNP or MAVRIC) is used for faster simulation and better convergence, grid geometry, which plays an important role in dose rates and convergence, should be specified carefully. It would be prudent to check some critical ADVANTG/MCNP results against analog MCNP results and similarly some critical MAVRIC results against analog Monaco results.

This study was performed for the ES-3100 package with different source configurations using HEU metal contents. For other packages where the geometric configuration is similar (except the content) and the detector locations are always on the package surfaces and at 1 m from the package surfaces, this paper can serve as a reference for SARP dose rate calculations with HEU contents. This work may be expanded in the future to address plutonium metal and oxide contents. Neutrons contribute a major portion of the total dose rates in plutonium contents whereas the neutron contribution in HEU contents is insignificant.

ACKNOWLEDGEMENTS

The author gratefully acknowledges the sincere support of Dr. Douglas E. Peplow of the Oak Ridge National Laboratory (ORNL) in developing the Monaco and MAVRIC models. The author also acknowledges Mr. James J. Yugo of the Y-12 National Security Complex (Y-12) and Dr. Scott W. Mosher of ORNL for their support in preparing ADVANTG input files and Mr. Richard W. Emmett of Y-12 for checking a select set of analog MCNP input/output files. Sincere acknowledgement goes to Mr. David A. Wilson of Navarro Research and Engineering and Ms. Becky Williams of Y-12 for technical editing and manuscript preparation of this paper. The author acknowledges Dr. Samuel N. Cramer of ORNL (retired) for exposing the author to shielding evaluation methodologies during the development of the ES-3100 package as well as introducing the capabilities of the MAVRIC and Monaco codes. The author also expresses his appreciation to Mr. Jeffrey. G. Arbital and James C. Anderson of Y-12 for arranging funding for this work at Y-12 under Contract DE-NA0001942.

REFERENCES

[1] Consolidated Nuclear Security, LLC, "Safety Analysis Report for Packaging, Y-12 National Security Complex, Model ES-3100 Package with Bulk HEU Contents," SP-PKG-801940-A001, Rev. 2, Page Change 1, Y-12 National Security Complex (June 2017).

[2] X-5 MONTE CARLO TEAM, "MCNP—A General Monte Carlo N-Particle Transport Code, Version 5, Volume I: Overview and Theory," LA-UR-03-1987, Los Alamos National Laboratory (April 2003, Revised February 2008).

[3] S. W. MOSHER et al., "ADVANTG—An Automated Variance Reduction Parameter Generator," ORNL/TM-2013/416, Oak Ridge National Laboratory (November 2013); https://doi.org/10.2172/1105937.

[4] "Scale*:* A Comprehensive Modeling and Simulation Suite for Nuclear Safety Analysis and Design," ORNL/TM-2005/39, Ver. 6.1, see also CCC-785, Radiation Safety Information Computational Center at Oak Ridge National Laboratory (June 2011). Denovo, KENO-VI, MAVRIC, Monaco, and ORIGEN-S codes are part of Scale.

[5] T. E. EVANS, A. S. STAFFORD, R. N. SLAYBAUGH, and K. T. CLARNO, "DENOVO: A New Three-Dimensional Parallel Discrete Ordinates Code in SCALE," *Nucl. Technol.*, **171**, *2*, 171 (2010); https://doi.org/10.13182/NT171-171.

[6] U.S. Nuclear Regulatory Commission, Title 10, *Code of Federal Regulations*, Part 71, *Packaging and Transportation of Radioactive Material*, Washington, DC (2018).

[7] U.S. Department of Transportation, Title 49, *Code of Federal Regulations*, Parts 100-178, *Transportation*, Washington, DC (2017).

[8] D. E. PEPLOW, "Monte Carlo Shielding Analysis Capabilities with MAVRIC," *Nucl. Technol.*, **174**, *2*, 289, (2011); https://doi.org/10.13182/NT174-289.

[9] J. C. WAGNER, D. E. PEPLOW, and S. W. MOSHER, "FW-CADIS Method for Global and Regional Variance Reduction of Monte Carlo Radiation Transport Calculations," *Nucl. Sci. Eng.*, **176**, *1*, 37 (2014); https://doi.org/10.13182/NSE12-33.

[10] D. E. PEPLOW, T. M. EVANS, and J. C. WAGNER, "Simultaneous Optimization of Tallies in Difficult Shielding Problems," *Nucl. Technol.*, **168**, *3*, 785 (2009); https://doi.org/10.13182/NT09-9.